arXiv:1212.3285v1 [cond-mat.mes-hall] 13 Dec 2012

Surface State Quasiparticle Interference in Crystalline Topological Insulators

Chen Fang[1,2], Matthew J. Gilbert[3,4], Su-Yang Xu [2], B. Andrei Bernevig[2], M. Zahid Hasan[2]
[1]*Department of Physics, University of Illinois, Urbana IL 61801-3080*
[2]*Department of Physics, Princeton University, Princeton NJ 08544*
[3]*Department of Electrical and Computer Engineering, University of Illinois, Urbana IL 61801 and*
[4]*Micro and Nanotechnology Laboratory, University of Illinois, Urbana IL 61801*
(Dated: December 14, 2012)

We theoretically study the quasiparticle interference (QPI) of the surface states in crystalline topological insulators which possess mirror symmetry and time-reversal symmetry, by analyzing the Fourier transformed local density of states (FT-LDOS), $\rho(\mathbf{q},\omega)$ around a single static impurity on the surface. We show that the symmetries in the QPI pattern are determined by the transformation properties of the impurity under mirror reflections and time-reversal. We study the singularities in $\rho(\mathbf{q},\omega)$ and show that while the presence of singularities in $\rho(\mathbf{q},\omega)$ depends on the geometric features of the iso-energy contour at ω, the *absence* of certain singularities denotes the scattering forbidden by underlying symmetries. We apply the general analysis to the QPI on the $\langle 001\rangle$-surface of $\mathrm{Pb}_{1-x}\mathrm{Sn}_x\mathrm{Te}$ and predict all vanishing singularities in $\rho(\mathbf{q},\omega)$. The model-independent analysis is supported by numerical calculations of $\rho(\mathbf{q},\omega)$ around a single point charge impurity using an effective four-band model. We demonstrate that QPI can also be used to probe the Lifshitz transition of the surface states observed in recent ARPES experiment.

Recent progress in topological materials indicates that topological states protected by time-reversal symmetry (TRS) may be the first identified class amongst a much wider family of topological states protected by discrete symmetries[1–7]. Hsieh *et al* predicted[5], via first principles calculation, that SnTe is a nontrivial insulator whose topological state is protected by mirror symmetries about $\langle 110\rangle$-planes. The physical manifestation of this nontrivial topological state is the existence of surface states on the $\langle 001\rangle$-plane which contains four Dirac points (two along $\bar{X}$-$\bar{\Gamma}$-$\bar{X}$ and two along $\bar{Y}$-$\bar{\Gamma}$-$\bar{Y}$). This prediction has been experimentally confirmed[8–10] through the use of angle resolved photoemission spectroscopy (ARPES) which has successfully identified the predicted surface states in $\mathrm{Pb}_{1-x}\mathrm{Sn}_x\mathrm{Te}$ and SnTe. It was also explicitly shown[8,10] that as the binding energy increases away from the Dirac point binding energy, the surface states undergo a Lifshitz transition at a critical energy E_c where the Fermi surface (FS) changes from two separate ellipsoids to two concentric ellipsoids.

While ARPES has established the existence of the nontrivial surface states and their dispersion, the information of the wave functions is missing; quasiparticle interference (QPI) study is a useful way to elucidate this information via scanning tunneling microscopy[11–16]. In this paper, we theoretically examine the symmetry protected features in the Fourier transformed local density of states (FT-LDOS) around a point impurity, $\rho(\mathbf{q},\omega)$. We analyze the general symmetries of $\rho(\mathbf{q},\omega)$, by examining the relations among the values of the FT-DOS at (q_x,q_y), $(q_x,-q_y)$ and $(-q_x,q_y)$, for all types of *static point impurities.* We predict the absence of symmetry forbidden singularities in $\rho(\mathbf{q},\omega)$. Generically the singularities are given by the *stationary points* on the iso-energy contour[17]. The *absence* of any of these singularities is determined by the orthogonality of wavefunctions at the corresponding stationary points, and is a symmetry protected property inherent to the system. We apply this result to $\mathrm{Pb}_{1-x}\mathrm{Sn}_x\mathrm{Te}$. We design a four-band model having all the symmetries of $\mathrm{Pb}_{1-x}\mathrm{Sn}_x\mathrm{Te}$ and capturing the overall features of the observed band structure. We calculate the FT-LDOS around a point charge impurity. Within the calculated $\rho(\mathbf{q},\omega)$, we can identify each singularity with a pair of stationary points on the iso-energy contour while symmetry forbidden singularities vanish. The QPI pattern changes drastically at the Lifshitz transition.

We begin by considering a bulk 3D insulator whose surface is terminated on the $\langle 001\rangle$-plane leaving only the in-plane momenta k_x and k_y as well-defined. Before turning to the study of any specific material, we want to understand the general features of $\rho(\mathbf{q},\omega)$ around a point impurity in the resultant 2D system having the three symmetries: mirror reflections about xz- and yz-planes and TRS. The three symmetries transform the single-particle Hamiltonian, $H(\mathbf{k})$, are defined as, $M_{xz}H(k_x,k_y)M_{xz}^{-1}=H(k_x,-k_y)$, $M_{yz}H(k_x,k_y)M_{yz}^{-1}=H(-k_x,k_y)$, $U_TH(k_x,k_y)U_T^{-1}=H^T(-k_x,-k_y)$, where $H(\mathbf{k})$ is written in a predefined but arbitrary orbital basis and M_x, M_y and U_T ($T=KU_T$) are the unitary matrices representing the symmetry operations in the same basis. U_T must be antisymmetric for a spinful system. We use the exact formulation of T-matrix to calculate $\rho(\mathbf{q},\omega)$ associated with any type of single impurities. We may express $\rho(\mathbf{q},\omega)$ in terms of the single particle retarded Green's function and its complex conjugate[18,19]:

$$\rho(\mathbf{q},\omega)= \\ -\frac{1}{N\pi}\sum_{\mathbf{k}}Tr[G(\mathbf{k},\mathbf{k}+\mathbf{q},\omega)-G^*(\mathbf{k}+\mathbf{q},\mathbf{k},\omega)], \quad (1)$$

where N is the total number of sites on the surface. The retarded Green's function $G(\mathbf{k}, \mathbf{k}+\mathbf{q}, \omega)$ given by

$$G(\mathbf{k}, \mathbf{k}+\mathbf{q}, \omega) = \\ G_0(\mathbf{k}, \omega)\delta_{\mathbf{q}0} + G_0(\mathbf{k}, \omega)T(\omega)G_0(\mathbf{k}+\mathbf{q}, \omega), \qquad (2)$$

where $G_0(\mathbf{k}, \omega) = (\omega - H(\mathbf{k}) + i\eta)^{-1}$, is the retarded Green's function for a homogenous system. The matrix $T(\omega)$ contains the effect of impurity and is defined as

$$T(\omega) = V(I - g(\omega)V)^{-1}, \qquad (3)$$

where V is the impurity potential matrix written in the orbital basis and $g(\omega) = \sum_{\mathbf{k}} G_0(\mathbf{k}, \omega)/N$. A necessary step in understanding the FT-LDOS is to examine the symmetries of $\rho(\mathbf{q}, \omega)$ by utilizing the symmetries of $H(\mathbf{k})$ and V. We do not *a priori* assume any symmetry for the static impurity potential V. Nevertheless, any V is capable of being decomposed into superposition of eight types of static impurities. Each type is marked by three Z_2-indices, $\eta = (\eta_x, \eta_y, \eta_T)$ which we define as $M_{xz}VM_{xz}^{-1} = \eta_x V$, $M_{yz}VM_{yz}^{-1} = \eta_y V$ and $U_T V U_T^{-1} = \eta_T V^T$. Each unique combination of Z_2-indices represents a particular type of impurity. For example, $\eta = (1, 1, 1)$ describes a static point charge impurity, invariant under both mirror reflections and TRS. The combination $\eta = (1, -1, 1)$ is an impurity invariant under mirror reflection about xz-plane and TRS yet changing sign under a mirror reflection about yz-plane. The physical realization for this combination of indices is an electric dipole which is oriented along x-axis. From these symmetries, we derive the exact and approximate symmetries of $\rho(\mathbf{q}, \omega)$ and summarize them in Table.I (for derivation, see Supplementary Materials). Here, 'approximate' means it is valid only when $||g(\omega)V||$ is small enough in the weak impurity limit.

Besides the global symmetries in $\rho(\mathbf{q}, \omega)$ derived above, the most important features of the FT-LDOS is the presence of singularities at certain $\mathbf{q}$-vectors. We start from writing $G(\mathbf{k}, \omega)$ in terms of projectors:

$$Tr[G(\mathbf{k}, \mathbf{k}+\mathbf{q}, \omega)] = \\ \sum_{mn} \frac{Tr[P_n(\mathbf{k}+\mathbf{q})P_m(\mathbf{k})T(\omega)]}{(\omega - E_m(\mathbf{k}) + i\eta)(\omega - E_n(\mathbf{k}+\mathbf{q}) + i\eta)}, \qquad (4)$$

where n is the band index and $P_n = |u_n(\mathbf{k})\rangle\langle u_n(\mathbf{k})|$ is the projector onto the n-th band. In Eq.(4), we have ignored a term $Tr[G_0(\mathbf{k}, \omega)]\delta_{\mathbf{q}0}$, which only contributes to the uniform part of DOS. The numerator on the RHS of Eq.(4) depends on the wave functions at $\mathbf{k}$ and $\mathbf{k}+\mathbf{q}$, while the denominator solely depends on the band dispersion. The major contribution to this quantity comes from states that are close to the energy contours as defined by $E_m(\mathbf{k}) = \omega$ and $E_n(\mathbf{k}+\mathbf{q}) = \omega$, corresponding to $\mathbf{k}$-points where the denominator almost vanishes. Specially, we expect $\rho(\mathbf{q}, \omega)$ to diverge at $\mathbf{q} = \mathbf{q}_s$ if at some $\mathbf{k}_{s1}$, we have: (i) $E_m(\mathbf{k}_{s1}) = E_n(\mathbf{k}_{s2} = \mathbf{k}_{s1} + \mathbf{q}) = \omega$ and (ii) the tangential lines of the iso-energy contours at $\mathbf{k}_{s1}$ and $\mathbf{k}_{s2}$ are parallel. Under these conditions, $\mathbf{k}_{s1,s2}$ are referred to as a pair of *stationary points*. However, through Eq.(4), we notice that a singularity at $\mathbf{q}_s = \pm(\mathbf{k}_{s1} - \mathbf{k}_{s2})$ only exists when the numerator, $Tr[P_j(\mathbf{k}_{s2})P_i(\mathbf{k}_{s1})T(\omega)]$ is *nonzero*. Therefore, if the two eigenstates $|u_m(\mathbf{k}_{s1})\rangle$ and $|u_n(\mathbf{k}_{s2})\rangle$ are orthogonal to one another, we have $P_m(\mathbf{k}_{s1})P_n(\mathbf{k}_{s2}) = 0$ and the corresponding singularity in FT-LDOS at $\mathbf{q}_s$ must vanish. In this way, we find that the *absence* of singularities in the FT-LDOS pattern is a symmetry protected property of the system, because in general $\langle u_m(\mathbf{k}_{s1})|u_n(\mathbf{k}_{s2})\rangle = 0$ can only be guaranteed by the presence of an underlying symmetry. One may compare the expression of $\rho(\mathbf{q}, \omega)$ in Eq.(1, 4) with that of the joint density of states at $\mathbf{q}$

(η_x, η_y, η_T)	Realization	Exact symmetries	Approximate relations	$\Sigma_{\alpha\beta}$
(1,1,1)	Point charge	$\rho(q_x, q_y) = \rho(-q_x, q_y)$ $\rho(q_x, q_y) = \rho(q_x, -q_y)$		$\Sigma_{00}, \Sigma_{10}, \Sigma_{30}$
(−1,1,1)	Electric dipole	$\rho(q_x, q_y) = \rho(-q_x, q_y)$	$\rho(q_x, q_y) \sim -\rho(q_x, -q_y)$	Σ_{23}
(1,−1,1)	Electric dipole 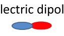	$\rho(q_x, q_y) = \rho(q_x, -q_y)$	$\rho(q_x, q_y) \sim -\rho(-q_x, q_y)$	Σ_{21}
(−1,−1,1)	Electric quadruple	$\rho(q_x, q_y) = \rho(-q_x, -q_y)$	$\rho(q_x, q_y) \sim -\rho(q_x, -q_y)$ $\rho(q_x, q_y) \sim -\rho(-q_x, q_y)$	Σ_{22}
(1,1,−1)	Magnetic quadruple	$\rho(q_x, q_y) = \rho(-q_x, q_y)$ $\rho(q_x, q_y) = \rho(q_x, -q_y)$	$\rho(q_x, q_y) \sim 0$	Σ_{20}
(−1,1,−1)	Point spin	$\rho(q_x, q_y) = \rho(-q_x, q_y)$ $\rho(q_x, q_y) = \rho(q_x, -q_y)$		$\Sigma_{03}, \Sigma_{13}, \Sigma_{33}$
(1,−1,−1)	Point spin	$\rho(q_x, q_y) = \rho(-q_x, q_y)$ $\rho(q_x, q_y) = \rho(q_x, -q_y)$		$\Sigma_{01}, \Sigma_{11}, \Sigma_{31}$
(−1,−1,−1)	Point spin	$\rho(q_x, q_y) = \rho(-q_x, -q_y)$		$\Sigma_{02}, \Sigma_{12}, \Sigma_{32}$

TABLE I. Different types of point impurities classified by whether they change signs under mirror symmetries and TRS. From the left: the η-index, the possible physical realization, the exact symmetries of $\rho(\mathbf{q}, \omega)$, the approximate symmetries of $\rho(\mathbf{q}, \omega)$ to the first order of V and the corresponding $\Sigma_{\alpha\beta}$ in the four-band effective model (see text).

$$\rho_J(\mathbf{q}, \omega) = \qquad (5) \\ -\frac{2}{N\pi}\mathrm{Im}[\sum_{m,n,\mathbf{k}} \frac{1}{(\omega - E_m(\mathbf{k}) + i\eta)(\omega - E_n(\mathbf{k}+\mathbf{q}) + i\eta)}].$$

One can see that the only difference is that in $\rho_J(\mathbf{q}, \omega)$ the factor $Tr[P_m(\mathbf{k})T(\omega)P_n(\mathbf{k}+\mathbf{q})]$ is missing. Hence $\rho_J(\mathbf{q}, \omega)$ is completely determined by the geometric features of the iso-energy contour: at every wave vector $\mathbf{q}$ joining two stationary points, there is an intensity peak in $\rho_J(\mathbf{q}, \omega)$. A comparison between $\rho(\mathbf{q}, \omega)$ and $\rho_J(\mathbf{q}, \omega)$ thus gives information of the wave functions, because any stationary vector that is present in the latter but absent in the former indicates that the two wave functions at the contributing stationary points are orthogonal[11].

In a system with M_{xz}, M_{yz} and TRS symmetries, there are three types of symmetry protected orthogonality: TRS gives us the orthogonality between two states of a Kramer's pair; M_{xz} (M_{yz}) ensures the orthogonality between two states with *different* eigenvalues of M_{xz} (M_{yz}). The orthogonality provided by TRS leads to the *forbidden back scattering* which is a hallmark of TRS topological materials. The orthogonality ensured by mirror symmetries, however, leads to new forbidden scattering channels. In order to identify them, we need the mirror eigenvalues of the surface states on an iso-energy contour. As an example, we obtain these values here for $\mathrm{Pb}_{1-x}\mathrm{Sn}_x\mathrm{Te}$. For the mirror reflection symmetry about xz-plane, we have $[M_{xz}, H(k_x, 0)] = [M_{xz}, H(k_x, \pi)] = 0$, therefore each band along $\bar{\Gamma}\bar{X}$ or $\bar{Y}\bar{M}$ may be labeled by its M_{xz} eigenvalue, either $+i$ or $-i$. Along the $\bar{\Gamma}\bar{X}/\bar{Y}\bar{M}$ direction, two bands with the *opposite* M_{xz} eigenvalues can cross each other as a gap opening in the bands is forbidden by the mirror symmetry (Fig.1(a)). Along $\bar{\Gamma}\bar{Y}/\bar{X}\bar{M}$-direction, each band can similarly be labeled by its M_{yz} eigenvalue, and along the $\bar{X}\bar{M}$ direction (k_y-direction), two bands are allowed to cross each other only if they have *opposite* eigenvalues of M_{yz}. The two Dirac nodes at $\bar{X}$ (marked by $D_{3,4}$) are protected by TRS and therefore appear in both directions; the other two Dirac nodes, $D_{1,2}$ are protected only by M_{xz} symmetry if they have *opposite* eigenvalues of M_{xz}. On the other hand, from the absence of Dirac nodes along $\bar{X}\bar{M}/\bar{\Gamma}\bar{Y}$ and that the two bands bend away from each other, they can either have the same eigenvalues of M_{yz} and hence repel each other (Fig.1(b)), or they can have the same eigenvalue of M_{yz} but opposite effective mass (Fig.1(c)). We only know that the two bands crossing at $D_{3,4}$ must have opposite M_{xz} eigenvalues. To see the Lifshitz transition, we find that for $E_{2c} < \omega < E_{1c}$, the bands along $\bar{X}\bar{M}$ do not cross ω, resulting in an iso-energy contour of two separate ellipsoids centered at $D_{1,2}$ respectively. From Fig.1(a), along $\bar{X}\bar{\Gamma}$, the two points on the same side of $\bar{X}$ have opposite eigenvalues of M_{xz}. While for $\omega > E_{c1}$ or $\omega < E_{c2}$, the bands along $\bar{X}\bar{M}$ cross ω twice, resulting in an iso-energy contour of two concentric loops centered at $\bar{X}$. From Fig.1(b, c), along $\bar{X}\bar{M}$, the two points on the same side of $\bar{X}$ have the same eigenvalues of M_{yz}.

To understand how this symmetry based QPI analysis applies to the FT-LDOS for $\mathrm{Pb}_{1-x}\mathrm{Sn}_x\mathrm{Te}$, we consider the iso-energy contour before the Lifshiitz transition, shown in Fig.1(d). Here $|u(\mathbf{k}_1)\rangle$ and $|u(\mathbf{k}_2)\rangle$, as well as $|u(\mathbf{k}_3)\rangle$ and $|u(\mathbf{k}_4)\rangle$, are eigenstates of M_{xz} each with different eigenvalues forcing them to be orthogonal. Now raise the energy, ω, such that we pass the critical point of the Lifshitz transition, as seen in Fig.1(e), where again $|u(\mathbf{k}'_1)\rangle$ and $|u(\mathbf{k}'_3)\rangle$ are orthogonal as are $|u(\mathbf{k}'_2)\rangle$ and $|u(\mathbf{k}'_4)\rangle$. On the other hand, along $\bar{\Gamma}\bar{Y}$, all of the states are eigenstates of M_{yz}, and $|u(\mathbf{k}'_5)\rangle$ and $|u(\mathbf{k}'_7)\rangle$ are orthogonal, while $|u(\mathbf{k}'_6)\rangle$ and $|u(\mathbf{k}'_8)\rangle$ are also orthogonal, because they each have different eigenvalues of M_{yz}. The vanishing singularities guaranteed by the mirror symmetries in $\rho(\mathbf{q}, \omega)$ are: $\mathbf{q}_{12}$, $\mathbf{q}_{34}$ and $\mathbf{q}_{23}$ before the Lifshitz transition ($\mathbf{q}_{ab}$ defined as $\mathbf{q}_a - \mathbf{q}_b$), and $\mathbf{q}_{1'2'}$, $\mathbf{q}_{3'4'}$, $\mathbf{q}_{2'3'}$, $\mathbf{q}_{5'7'}$, $\mathbf{q}_{6'7'}$ and $\mathbf{q}_{5'8'}$ after the Lifshitz transition. Mark that $\mathbf{q}_{14}$, $\mathbf{q}_{23}$, $\mathbf{q}_{1'4'}$, $\mathbf{q}_{2'3'}$, $\mathbf{q}_{5'8'}$, $\mathbf{q}_{6'7'}$ are also forbidden by TRS as they are scattering vectors connecting Kramer's pairs in the presence of TRS.

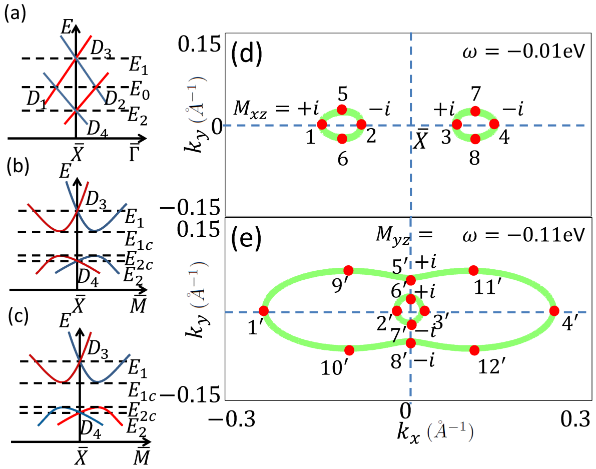

FIG. 1. Schematic band dispersion of the surface bands at vicinity of $\bar{X}$ along (a) k_x-axis and (b) k_y-axis. Red/blue (lighter/darker grey) means the band has eigenvalue $+i/-i$ of M_{xz} in (a) and M_{yz} in (b,c). Iso-energy contour calculated for the model described in the text at $\omega = -0.01$eV in (d) and $\omega = -0.11$eV in (e). Eigenvalues of M_{xz} at points $1, 2, 3, 4$ are marked beside each point, and eigenvalues of M_{yz} at points $5', 6', 7', 8'$ are similarly marked. The eigenvalues of M_{xz} at points $1', 2', 3', 4'$ are identical to those at $1, 2, 3, 4$.

Thus far, we have extracted the symmetries of the single impurity QPI pattern and located all vanishing singularities guaranteed by the presence of mirror symmetries, as one expects in $\mathrm{Pb}_{1-x}\mathrm{Sn}_x\mathrm{Te}$. However, in order to be more concrete, we develop a $\mathbf{k}\cdot\mathbf{p}$-model which qualitatively captures the surface band dispersion both before and after the Lifshitz transition and calculate the $\rho(\mathbf{q}, \omega)$ around a point impurity. Near the Dirac points $D_{1,2}$, the system can be approximated by two separate two-band $\mathbf{k}\cdot\mathbf{p}$ models. Nevertheless, in order to describe the Lifshitz transition where the two cones cross each other, one needs to consider the hybridization between the two cones and, thus, the two band model must expand to four as the minimal number of bands in the effective Hamiltonian. At $\bar{X}$ there are two degenerate states at D_3 with $E_1 > E_D$ and two other degenerate states at D_4 with $E_2 < E_D$. Within each doublet, one is an eigenstate of M_{xz} with an eigenvalue of $+i$ while the other $-i$. We thus select our basis to be: $(1, 0, 0, 0)$ and $(0, 1, 0, 0)^T$ with energy E_1 and mirror eigenvalues of $M_{yz} = +i$ and $M_{yz} = -i$ respectively; $(0, 0, 1, 0)^T$ and $(0, 0, 0, 1)^T$ with energy E_2 and similarly corresponding mirror eigenvalues of $M_{yz} = +i$ and $M_{yz} = -i$ respectively. There is a gauge freedom in choosing the matrices for M_{xz} and U_T under this basis, and we choose $M_{xz} = i\Sigma_{10}$ and $U_T = i\Sigma_{20}$, where $\Sigma_{\alpha\beta} = \sigma_\alpha \otimes \sigma_\beta$. Applying symmetry constraints, we find that, to the linear order in $\mathbf{k}$, Σ_{30} and Σ_{10} couple to the zeroth order, $\Sigma_{01,11,31}$ couple to k_x and $\Sigma_{03,13,33}$ couple to k_y. The effective Hamiltonian can hence be written as

$$\begin{aligned} H(\mathbf{k}) = m\Sigma_{30} + m'\Sigma_{10} + (v_{1x}\Sigma_{01} + v_{2x}\Sigma_{11} + v_{3x}\Sigma_{31})k_x \\ + (v_{1y}\Sigma_{03} + v_{2y}\Sigma_{13} + v_{3y}\Sigma_{33})k_y. \end{aligned} \tag{6}$$

Qualitatively fitting the data for $\mathrm{Pb}_{1-x}\mathrm{Sn}_x\mathrm{Te}$ given in Ref.[8], we choose the parameters in our Hamiltonian to be: $\{m, m'\} = \{-0.11, -0.1\}$eV, $\{v_{1x}, v_{2x}, v_{3y}\} = \{-1.5, -0.5, -3\}eV\cdot\mathring{A}$ and $\{v_{3x}, v_{1y}, v_{2y}\} \sim 0$. Here we define ~ 0 as a parameter that is very small but nonzero in order to avoid accidental symmetries. We represent V for impurities with different η-indices in a similar fashion using this basis, given in the last column of Table I.

Using the effective Hamiltonian for $\mathrm{Pb}_{1-x}\mathrm{Sn}_x\mathrm{Te}$, we calculate $\rho(\mathbf{q}, \omega)$ with $V = 0.1eV * \Sigma_{00}$, for a static point charge impurity, as this is the most likely impurity to be present in $\mathrm{Pb}_{1-x}\mathrm{Sn}_x\mathrm{Te}$. In Fig.2(b,d), we plot $|\nabla^2\rho(\mathbf{q}, \omega)|$ at $\omega = -0.01eV$ and $\omega = -0.11eV$ respectively. ($|\nabla^2\rho(\mathbf{q}, \omega)|$ is plotted in lieu of $\rho(\mathbf{q}, \omega)$ since it shows the singularities more clearly.) In comparison, we make the same plots for the joint density of states, $|\nabla^2\rho_J(\mathbf{q}, \omega)|$, in Fig.2(a, c). In Fig.2(a, c), we mark several $\mathbf{q}_s$'s that join stationary $\mathbf{k}$-points marked in Fig.1, and at all these vectors, there are peaks in $|\nabla^2\rho_J(\mathbf{q}, \omega)|$. However, in Fig.2(b, d), we see that all peaks that are forbidden by either TRS or mirror symmetries vanish, confirming the previous analysis based on mirror eigenvalues of the $\mathbf{k}$-points.

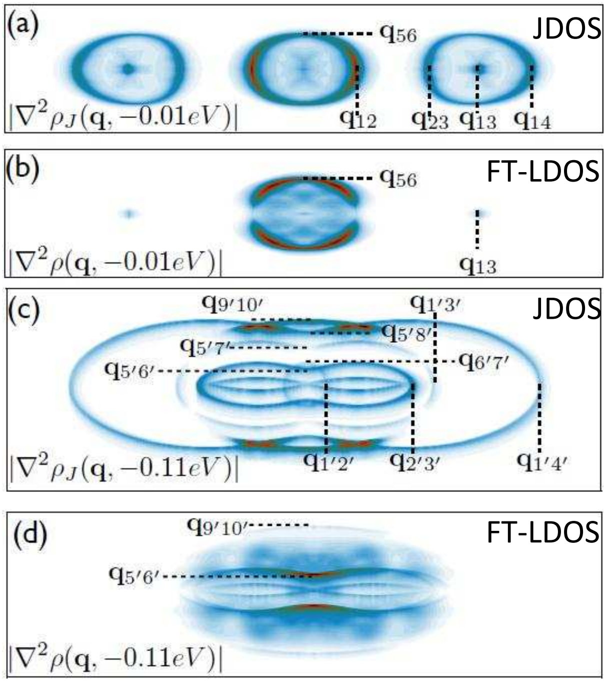

FIG. 2. The absolute value of the divergence of the joint density of states, $|\nabla^2\rho_J(\mathbf{q}, \omega)|$, is plotted for $\omega = -0.01$eV (a) and -0.11eV (c). The absolute value of the divergence of FT-LDOS around a static impurity potential $V = 0.1eV * \Sigma_{00}$, $|\nabla^2\rho(\mathbf{q}, \omega)|$, is plotted for $\omega = -0.01$eV (b) and -0.11eV (d).

$\rho(\mathbf{q}, \omega)$ as measured in $\mathrm{Pb}_{1-x}\mathrm{Sn}_x\mathrm{Te}$ may contain additional complications in identifying the crucial symmetry protected features of the QPI. The surface is considerably doped with Pb atoms then, if the scattering off of surface electrons by these atoms cannot be ignored, the QPI pattern is generated by many similar impurities instead of a single impurity. However, given the random distribution of impurities, one can measure the autocorrelation function of $R(\mathbf{r}, \omega)$, i.e., $C(\mathbf{r}, \omega) = \langle \int dr'^3 R(\mathbf{r}+\mathbf{r}', \omega) R(\mathbf{r}', \omega)\rangle$, where $R(\mathbf{r}, \omega)$ is the FT-LDOS contributed by *all* impurities and $\langle\rangle$ means the ensemble average over impurity configurations. As the Fourier transform of $C(\mathbf{r}, \omega)$ is simply proportional to $|\rho(\mathbf{q}, \omega)|^2$ to the lowest order of V (See Supplementary Materials), the QPI structure around a single impurity is reflected in the autocorrelation of the overall QPI pattern in the limit of weak and identical random impurities.

It is necessary to point out that we have assumed that $\rho(\mathbf{q}, \omega)$ contains contributions only from scattering between states near $\bar{X}$. However, the full QPI pattern also consists of the scattering among states near $\bar{Y}$ and the inter-pocket scattering between states near $\bar{X}$ and those near $\bar{Y}$. Yet due to C_4-symmetry, the contribution to $\rho(\mathbf{q}, \omega)$ made by states near $\bar{Y}$ can be obtained easily by making a fourfold rotation of $\rho(\mathbf{q}, \omega)$ contributed by states around $\bar{X}$. The inter-scattering between states near $\bar{Y}$ and those near $\bar{X}$ only contributes to $\rho(\mathbf{q}, \omega)$ at $\mathbf{q} \sim \bar{X} - \bar{Y} = (\pi, \pi)$. As these states are sufficiently separated in $\mathbf{q}$-space from features of in the small $\mathbf{q}$-region, they are be neglected in this work.

In samples with $x \sim 1$ or pure SnTe, a spontaneous lattice distortion break one of the mirror symmetries (assumed to be M_{yz}) and C_4 symmetry. Assuming that the distortion breaks M_{xz}, we know that: first, the two Dirac nodes along $\bar{\Gamma}\bar{X}$ are no longer protected and open a gap of $2E_D$; second, the Lifshitz transition happens at two different energies, E_{cx} and E_{cy}, for the surface states around $\bar{X}$ and around $\bar{Y}$. As energy decreases from E_f, there are four phases: (i) no FS around $\bar{X}$ and two ellipsoids around $\bar{X}$ when $|\omega| < E_D$, (ii) two ellipsoids of FS around $\bar{X}$ and two other around $\bar{Y}$ when $E_D < |\omega| < |E_{cy}|$, (iii) two ellipsoids around $\bar{X}$ and two concentric loops around $\bar{Y}$ if $|E_{cy}| < |\omega| < |E_{cx}|$ and (iv) two concentric loops around $\bar{X}$ and two others around $\bar{Y}$ if $|\omega| > |E_{cx}$. All these phases can be identified by QPI (see Supplementary Materials). In the pattern, all forbidden scattering vectors forbidden by M_{xz} are present while those forbidden by M_{yz} or TRS remain absent.

ACKNOWLEDGMENTS

CF is supported by ONR - N00014-11-1-0635. MJG acknowledges support from the AFOSR under grant FA9550-10-1-0459 and the ONR under grant N0014-11-1-0728. BAB was supported by NSF CAREER DMR-095242, ONR - N00014-11-1-0635, Darpa - N66001-11-1-4110, and David and Lucile Packard Foundation.

[1] A. P. Schnyder, S. Ryu, A. Furusaki, and A. W. W. Ludwig, Phys. Rev. B **78**, 195125 (2008).

[2] L. Fu, Phys. Rev. Lett. **106**, 106802 (2011).

[3] T. L. Hughes, E. Prodan, and B. A. Bernevig, Phys. Rev. B **83**, 245132 (2010).

[4] A. M. Turner, Y. Zhang, R. S. K. Mong, and A. Vishwanath, Phys. Rev. B **85**, 165120 (2012).

[5] T. Hsieh, H. Lin, J. Liu, W. Duan, A. Bansil, and L. Fu, Nature Communications **3**, 982 (2012).

[6] C. Fang, M. J. Gilbert, X. Dai, and B. A. Bernevig, Phys. Rev. Lett. **108**, 266802 (2012).

[7] C. Fang, M. J. Gilbert, and B. A. Bernevig, Phys. Rev. B **86**, 115112 (2012).

[8] S.-Y. Xu, C. Liu, N. Alidoust, D. Qian, M. Neupane, J. D. Denlinger, Y. J. Wang, L. A. Wray, R. J. Cava, H. Lin, A. Marcinkova, E. Morosan, A. Bansil, and M. Z. Hasan, Nature Communications **3**, 1192 (2012).

[9] P. Dziawa, B. J. Kowalski, K. Dybko, R. Buczko, A. Szczerbakow, M. Szot, E. Ausakowska, T. Balasubramanian, B. M. Wojek, M. H. Berntsen, O. Tjernberg, and T. Story, Nature Materials **advance online publication** (2012).

[10] T. Tanaka, Z. Ran, T. Sato, K. Nakayama, S. Souma, T. Takahashi, K. Segawa, and Y. Ando, Nature Physics **advance online publication** (2012).

[11] P. Roushan, J. Seo, C. V. Parker, Y. S. Hor, D. Hsieh, D. Qian, A. Richardella, M. Z. Hasan, R. J. Cava, and A. Yazdani, Nature **460**, 1106 (2009).

[12] T. Zhang, P. Cheng, X. Chen, J.-F. Jia, X. Ma, K. He, L. Wang, H. Zhang, X. Dai, Z. Fang, X. Xie, and Q.-K. Xue, Phys. Rev. Lett. **103**, 266803 (2009).

[13] J. Seo, P. Roushan, H. Beidenkopf, Y. S. Hor, R. J. Cava, and A. Yazdani, Nature **466**, 343 (2010).

[14] Y. Okada, C. Dhital, W. Zhou, E. D. Huemiller, H. Lin, S. Basak, A. Bansil, Y.-B. Huang, H. Ding, Z. Wang, S. D. Wilson, and V. Madhavan, Phys. Rev. Lett. **106**, 206805 (2011).

[15] Z. Alpichshev, J. G. Analytis, J.-H. Chu, I. R. Fisher, Y. L. Chen, Z. X. Shen, A. Fang, and A. Kapitulnik, Phys. Rev. Lett. **104**, 016401 (2010).

[16] Z. Alpichshev, J. G. Analytis, J.-H. Chu, I. R. Fisher, and A. Kapitulnik, Phys. Rev. B **84**, 041104 (2011).

[17] Q. Liu, X.-L. Qi, and S.-C. Zhang, Phys. Rev. B **85**, 125314 (2012).

[18] X. Zhou, C. Fang, W.-F. Tsai, and J. Hu, Phys. Rev. B **80**, 245317 (2009).

[19] W.-C. Lee, C. Wu, D. P. Arovas, and S.-C. Zhang, Phys. Rev. B **80**, 245439 (2009).

I. DERIVATION OF THE GLOBAL SYMMETRIES OF $\rho(\mathbf{q},\omega)$ FOR DIFFERENT TYPES OF SINGLE IMPURITIES

In this section we explicitly derive the symmetries of $\rho(\mathbf{q},\omega)$, exact and approximate, listed in Table I of the main text for single impurities with eight possible η-indices.

From Eq.(1), $\rho(\mathbf{q},\omega)$ is determined by the retarded Green's function $G(\mathbf{k},\mathbf{k}+\mathbf{q},\omega)$; yet from Eq.(2), $G(\mathbf{k},\mathbf{k}+\mathbf{q},\omega)$ is given in terms of the free particle Green's function $G_0(\mathbf{k},\omega)$ and the T-matrix, $T(\omega)$. The former has exactly the same symmetries as the homogenous Hamiltonian:

$$\begin{aligned} M_{xz}G_0(k_x,k_y,\omega)M_{xz}^{-1} &= G_0(k_x,-k_y,\omega), \\ M_{yz}G_0(k_x,k_y,\omega)M_{yz}^{-1} &= G_0(-k_x,k_y,\omega), \\ U_TG_0(\mathbf{k},\omega)U_T^{-1} &= G_0^T(-\mathbf{k},\omega). \end{aligned} \tag{7}$$

The symmetries of $T(\omega)$, however, depends on symmetries of both the system *and* the impurity, i.e., the η-index. Using definitions of η-index and Eq.(3), one obtains:

$$\begin{aligned} M_{xz}T(\omega)M_{xz}^{-1} = \eta_xV(I-\eta_xg(\omega)V)^{-1} &= T(\omega) \text{ if } \eta_x=1, \\ &\sim -T(\omega) \text{ if } \eta_x=-1, \\ M_{yz}T(\omega)M_{yz}^{-1} = \eta_yV(I-\eta_yg(\omega)V)^{-1} &= T(\omega) \text{ if } \eta_y=1, \\ &\sim -T(\omega) \text{ if } \eta_y=-1, \\ U_TT(\omega)U_T^{-1} = (\eta_TV(I-\eta_Tg(\omega)V)^{-1})^T &= T^T(\omega) \text{ if } \eta_T=1, \\ &\sim -T^T(\omega) \text{ if } \eta_T=-1. \end{aligned} \tag{8}$$

Here '$\sim$' means that the relation becomes exact only if $T(\omega)$ is replaced by its leading order, i.e., $T=V$.

Combining equations in Eqs.(8), one easily obtains other two equations:

$$\begin{aligned} (M_{xz}M_{yz})T(\omega)(M_{xz}M_{yz})^{-1} = \eta_x\eta_yV(I-\eta_x\eta_yg(\omega)V)^{-1} &= T(\omega) \text{ if } \eta_x\eta_y=1, \\ &\sim -T(\omega) \text{ if } \eta_x\eta_y=-1, \end{aligned} \tag{9}$$

$$\begin{aligned} (M_{xz}M_{yz}U_T)T(\omega)(M_{xz}M_{yz}U_T)^{-1} = [\eta_x\eta_y\eta_TV(I-\eta_x\eta_y\eta_Tg(\omega)V)^{-1}]^T &= T^T(\omega) \text{ if } \eta_x\eta_y\eta_T=1 \\ &\sim -T^T(\omega) \text{ if } \eta_x\eta_y\eta_T=-1. \end{aligned} \tag{10}$$

Now we use Eqs.(7) and Eqs.(8) and have

$$\begin{aligned}\rho(q_x,q_y,\omega) &= \frac{1}{N\pi}\sum_{\mathbf{k}}[Tr(M_{xz}G_0(k_x,k_y,\omega)T(\omega)G_0(k_x+q_x,k_y+q_y,\omega)M_{xz}^{-1}) - (\mathbf{q}\to-\mathbf{q})^*] \\ &= \frac{1}{iN\pi}\sum_{\mathbf{k}}[Tr(G_0(k_x,k_y,\omega)M_{xz}T(\omega)M_{xz}^{-1}G_0(k_x+q_x,k_y-q_y,\omega)) - (\mathbf{q}\to-\mathbf{q})^*] \\ &= \rho(q_x,-q_y,\omega) \text{ if } \eta_x = 1 \\ &\sim -\rho(q_x,-q_y,\omega) \text{ if } \eta_x = -1,\end{aligned} \tag{11}$$

$$\begin{aligned}\rho(q_x,q_y,\omega) &= \frac{1}{iN\pi}\sum_{\mathbf{k}}[Tr(M_{yz}G_0(k_x,k_y,\omega)T(\omega)G_0(k_x+q_x,k_y+q_y,\omega)M_{yz}^{-1}) - (\mathbf{q}\to-\mathbf{q})^*] \\ &= \frac{1}{iN\pi}\sum_{\mathbf{k}}[Tr(G_0(k_x,k_y,\omega)M_{yz}T(\omega)M_{yz}^{-1}G_0(k_x-q_x,k_y+q_y,\omega)) - (\mathbf{q}\to-\mathbf{q})^*] \\ &= \rho(-q_x,q_y,\omega) \text{ if } \eta_y = 1 \\ &\sim -\rho(-q_x,q_y,\omega) \text{ if } \eta_y = -1,\end{aligned} \tag{12}$$

$$\begin{aligned}\rho(q_x,q_y,\omega) &= \frac{1}{iN\pi}\sum_{\mathbf{k}}[Tr(U_TG_0(k_x,k_y,\omega)T(\omega)G_0(k_x+q_x,k_y+q_y,\omega)U_T^{-1}) - (\mathbf{q}\to-\mathbf{q})^*] \\ &= \frac{1}{iN\pi}\sum_{\mathbf{k}}[Tr(G_0(-k_x-q_x,-k_y-q_y,\omega)(U_TT(\omega)U_T^{-1})^TG_0(-k_x,-k_y,\omega)) - (\mathbf{q}\to-\mathbf{q})^*] \\ &= \frac{1}{iN\pi}\sum_{\mathbf{k}}[Tr(G_0(k_x-q_x,k_y-q_y,\omega)(U_TT(\omega)U_T^{-1})^TG_0(k_x,k_y,\omega)) - (\mathbf{q}\to-\mathbf{q})^*] \\ &= \rho(q_x,q_y,\omega) \text{ if } \eta_T = 1 \\ &\sim -\rho(q_x,q_y,\omega) \text{ if } \eta_T = -1.\end{aligned} \tag{13}$$

We can also use Eqs.(7) and Eqs.(9) to obtain, very similarly,

$$\begin{aligned}\rho(q_x,q_y,\omega) &= \rho(-q_x,-q_y,\omega) \text{ if } \eta_x\eta_y = 1 \\ &\sim -\rho(-q_x,-q_y,\omega) \text{ if } \eta_x\eta_y = -1,\end{aligned} \tag{14}$$

$$\begin{aligned}\rho(q_x,q_y,\omega) &= \rho(-q_x,-q_y,\omega) \text{ if } \eta_x\eta_y\eta_T = 1 \\ &\sim -\rho(-q_x,-q_y,\omega) \text{ if } \eta_x\eta_y\eta_T = -1.\end{aligned} \tag{15}$$

Up to now we have derived all symmetries, exact and approximate, of $\rho(\mathbf{q},\omega)$ listed in Table I.

II. AUTOCORRELATION OF $R(\mathbf{r},\omega)$ IN THE WEAK IMPURITY LIMIT

In the text, we mention that although we have only studied the case of a single impurity, the result extends to the case where there are random impurities of the same type and strength and when the impurity strength is weak. Here we prove that under these conditions, the FT-LDOS around a single impurity, $\rho(\mathbf{q},\omega)$, can be related to the autocorrelation function of the overall LDOS resulted from many impurities, $R(\mathbf{r},\omega)$. By definition,

$$R(\mathbf{r},\omega) = \sum_n |\psi_n(\mathbf{r})|^2\delta(\omega-E_n) = -\frac{1}{\pi}Im[G(\mathbf{r},\mathbf{r},\omega)], \tag{16}$$

where $\psi_n(\mathbf{r})$ is an eigenfunction of the Hamiltonian, having eigenvalue E_n. The Fourier transform of $R(\mathbf{r})$ is, in terms of the retarded Green's function,

$$R(\mathbf{q},\omega) = \frac{1}{N\pi}\sum_{\mathbf{k}} Tr[G(\mathbf{k},\mathbf{k}+\mathbf{q},\omega) - G^*(\mathbf{k}+\mathbf{q},\mathbf{k},\omega)], \tag{17}$$

which is identical to the expression of $\rho(\mathbf{r})$ in the case of a single impurity. But now $G(\mathbf{k},\mathbf{k}+\mathbf{q},\omega)$ does not have a simple expression as in Eq.(3) in the text, since the system contains more than one impurity.

By definition, we have the Fourier transform of the correlation function $C(\mathbf{r})$ as (from here, we suppress the argument of ω for concision)

$$\begin{aligned} C(\mathbf{q}) &= \frac{1}{(2\pi)^3 N}\int d^3r' d^3r \langle R(\mathbf{r}+\mathbf{r}')R(\mathbf{r}')\exp(-i\mathbf{q}\cdot\mathbf{r})\rangle \\ &= \langle |R(\mathbf{q})|^2\rangle. \end{aligned} \tag{18}$$

Therefore the Fourier transform of the autocorrelation function $C(\mathbf{r})$ is exactly the ensemble average of the module squared Fourier component $R(\mathbf{q})$.

For an arbitrary configuration of identical impurities, the retarded Green's function is

$$G(\mathbf{k},\mathbf{k}+\mathbf{q}) = G_0(\mathbf{k})\delta_{\mathbf{q}0} + G_0(\mathbf{k})V(\mathbf{q})G_0(\mathbf{k}+\mathbf{q}) + \frac{1}{N}\sum_{\mathbf{k}'} G_0(\mathbf{k})V(\mathbf{k}-\mathbf{k}')G_0(\mathbf{k}')V(\mathbf{k}'-\mathbf{k}-\mathbf{q})G_0(\mathbf{k}+\mathbf{q}) + ... \tag{19}$$

where $V(\mathbf{q}) = V\sum_i \exp(-i\mathbf{q}\cdot\mathbf{r}_i)$ is the Fourier transform of the impurity potential. From the above equation we have $R(\mathbf{q})$ as

$$R(\mathbf{q}) = \rho_0\delta_{\mathbf{q}0} + \frac{1}{iN}\sum_{\mathbf{k}} Tr[G_0(\mathbf{k})V(\mathbf{q})G_0(\mathbf{k}+\mathbf{q}) - G_0^*(\mathbf{k}+\mathbf{q})V(\mathbf{q})G_0^*(\mathbf{k})] \tag{20}$$

$$+\frac{1}{iN^2}\sum_{\mathbf{k},\mathbf{k}'}\sum_{\mathbf{k}} Tr[G_0(\mathbf{k})V(\mathbf{k}-\mathbf{k}')G_0(\mathbf{k}')V(\mathbf{k}'-\mathbf{k}-\mathbf{q})G_0(\mathbf{k}+\mathbf{q}) - G_0^*(\mathbf{k}+\mathbf{q})V(\mathbf{k}'-\mathbf{k}-\mathbf{q})G_0^*(\mathbf{k}')V(\mathbf{k}-\mathbf{k}')G_0^*(\mathbf{k})] + ...$$

For $\mathbf{q}\neq 0$, the lowest order in $|\rho(\mathbf{q})|^2$ is the second order in V:

$$\begin{aligned} |R(\mathbf{q})|^2 &= |Tr\{\frac{1}{N}\sum_{\mathbf{k}}[G_0(\mathbf{k})V(\mathbf{q})G_0(\mathbf{k}+\mathbf{q}) - G_0^*(\mathbf{k}+\mathbf{q})V(\mathbf{q})G_0^*(\mathbf{k})]\}|^2|\sum_i \exp(-i\mathbf{q}\cdot\mathbf{r}_i)|^2 \\ &= |\rho(\mathbf{q})|^2|\sum_i \exp(-i\mathbf{q}\cdot\mathbf{r}_i)|^2. \end{aligned} \tag{21}$$

Finally, we use the independence (randomness) of the distribution of $\mathbf{r}_i$ to prove that

$$\langle|\sum_i \exp(-i\mathbf{q}\cdot\mathbf{r}_i)|^2\rangle = N_i + \sum_{i\neq j}\langle\exp(i\mathbf{q}\cdot(\mathbf{r}_j-\mathbf{r}_i))\rangle = N_i,$$

where N_i is the total number of impurities. Up to this point, we have proved that Fourier transform of the autocorrelation function $C(\mathbf{r})$ of the overall LDOS $R(\mathbf{r})$ is proportional to $|\rho(\mathbf{q})|^2$ in the limit of weak impurities. In other words, the singularities in $\rho(\mathbf{q})$ can be revealed in the autocorrelation of LDOS in the case of multiple identical impurities.

III. QPI WITH RHOMBOHEDRAL DISTORTION

In the text, we have mentioned that QPI can be used to identify the four types of iso-energy contours at different energy ω. In this section we use the effective model as example to see how $\rho(\mathbf{q},\omega)$ evolves as ω varies.

Without loss of generality, we assume that the distortion breaks M_{xz} but preserves M_{yz} TRS. In the presence of the rhombohedral distortion, the fourfold rotation symmetry is broken and we have to consider the contribution from states near $\bar{X}$ and $\bar{Y}$ separately. Any term that breaks M_{xz} but preserves M_{yz} and TRS is of index $\eta = (-1,+1,+1)$. According to Table I, in the effective theory around $\bar{X}$, this term is $\Delta\Sigma_{23}$. Without distortion, the effective theory around $\bar{Y}$ is obtained by rotating the model in Eq.(6) by $\pi/2$, and in this theory, the distortion term corresponds to $\Delta\Sigma_{23}$. In Fig.3, we choose $\Delta = 0.1$eV and calculate the iso-energy contours at $\omega = -0.01$eV in (a), -0.07eV in (b), -0.11eV in (c) and -0.15eV in (d). From these figures, the change in the topology of the contours is clear: it changes from only two separate ellipsoids around $\bar{Y}$ in (a), to two separate ellipsoids around both $\bar{X}$ and $\bar{Y}$ in (b), to two separate ellipsoids around $\bar{X}$ and two concentric loops in (c), and finally to two concentric loops around both $\bar{X}$ and $\bar{Y}$ at highest ω in (d). The resultant QPI patterns, $|\nabla^2\rho(\mathbf{q},\omega)|$, at these energies are plotted in Fig.3(e, f, g, h) respectively. These patterns are simply superpositions of patterns contributed by states around $\bar{X}$ and those around $\bar{Y}$; each pattern explicitly breaks fourfold rotational symmetry. Another important feature is that all $\mathbf{q}$-vectors that are forbidden by M_{xz} are now present. For example, in Fig.3(f), the inner circle is contributed by the surface states around $\bar{X}$. On this circle, the left and right ends, defined as $\mathbf{q}_L$ and $\mathbf{q}_R$ are due to the scattering between $\mathbf{k}$'s at the two ends of either one of the two pockets near $\bar{X}$. When M_{xz} is unbroken, these two $\mathbf{k}$'s have opposite M_{xz} eigenvalues and hence scattering between them is forbidden. But with M_{xz} broken, $\mathbf{q}_{L,R}$ are allowed by symmetry. Compare this with Fig.1(b), we can see that the distortion makes the intensity at $\mathbf{q}_{L,R}$ finite.

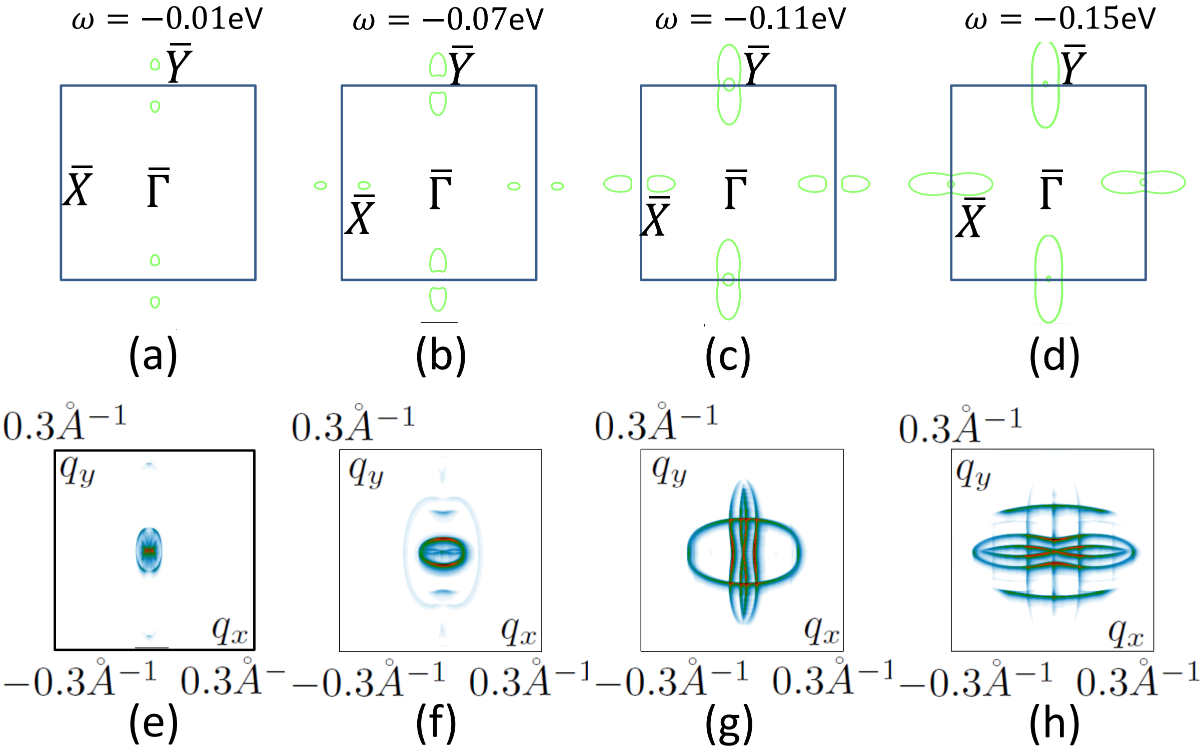

FIG. 3. (a,b,c,d): The iso-energy contours at $\omega = -0.01$eV, -0.07eV, -0.11eV and -0.15eV, respectively, in the phase with rhombohedral distortion, breaking M_{xz} symmetry. (e,f,g,h): $\nabla^2\rho(\mathbf{q},\omega)$ calculated for he surface states in the rhombohedral phase around a single charge impurity at the same energies listed above.